

Adaptive Ray Tracing for Radiative Transfer around Point Sources

Tom Abel^{1,2} and Benjamin D. Wandelt^{3,4,5}

¹ *Harvard Smithsonian Center for Astrophysics, Cambridge, MA, 02138, USA*

² *Institute of Astronomy, Madingley Road, Cambridge, CB03 0HA, UK*

³ *Department of Physics, Princeton University, Princeton, NJ 08544, USA*

⁴ *Department of Physics, University of Illinois, Urbana, IL 61801, USA*

⁵ *Department of Astronomy, University of Illinois, Urbana, IL 61801, USA*

revised manuscript of a Letter to the Editor for publication in MNRAS

ABSTRACT

We describe a novel adaptive ray tracing scheme to solve the equation of radiative transfer around point sources in hydrodynamical simulations. The angular resolution adapts to the local hydrodynamical resolution and hence is of use for adaptive meshes as well as adaptive smooth particle hydrodynamical simulations. Recursive creation of rays ensures ease of implementation. The multiple radial integrations needed to solve the time dependent radiative transfer are sped up significantly using a quad-tree once the rays are cast. Simplifications advantageous for methods with one radiation source are briefly discussed. The suggested method is easily generalized to speed up Monte Carlo radiative transfer techniques. In summary a nearly optimal use of long characteristics is presented and aspects of its implementation and comparison to other methods are given.

1 INTRODUCTION

Numerous questions in physical cosmology and galaxy formation require a detailed understanding of the physics of radiative transfer. Of particular interest are problems related to the reionization of the intergalactic medium (Haiman, Abel, and Madau 2000, Barkana and Loeb 2000, and references therein), absorption line signatures of high redshift structures (Kepner et al. 1999; Abel and Mo 1998). Hydrodynamic and thermal effects of UV emitting central sources on galaxy formation are also of interest (e.g. Haehnelt 1995; Silk and Rees 1998).

Consequently a number of methods for solving radiative transfer in three dimensional cosmological hydrodynamical simulations have been developed. Abel, Norman and Madau (1999, ANM99 hereafter) introduced a ray tracing scheme that employed rays of uniform angular resolution to solve the time dependent radiative transfer on uniform Cartesian grids for point sources. A related ray tracing approach was introduced by Razoumov and Scott (1999) which can also handle diffuse radiation fields but limited computer memory limits the angular resolution and therefore only poorly captures ionization fronts around point sources on reasonably large grids. Ciardi et al. (2001) discuss a Monte Carlo approach to sample angles, energies and the time evolution of the radiative transfer problem. Such Monte Carlo techniques may be able to use aspects of our new method to choose a more optimal number of photon packets. A ray-tracing scheme for use with Smooth Particle Hydrodynamics was introduced by Kessel-Deynet and Burkert (2000). Moment methods using variable Eddington tensors in three dimen-

sions have been suggested by (Norman, Paschos, and Abel 1998) and implemented (Gnedin and Abel 2001). Please note that there is much more literature on the problem of radiative transfer in two dimensions (c.f. Turner and Stone 2001, and references therein).

In this Letter we introduce a novel adaptive ray tracing scheme which is applicable for solving any line integrals on radial rays on uniform and adaptive Cartesian grids as well as particle methods.

The algorithm and aspects of an implementation are explained in the following section. Section 3 gives an illustrative example application. In the discussion section 4 we outline strategies to adapt our method to some particular applications of interest.

2 METHOD

2.1 Illustrative Problem

To motivate and introduce the new method we consider the specific example problem of solving the monochromatic radiative transfer of Lyman continuum photons from an isotropic point source photo-ionizing a neutral hydrogen density distribution, $n_H(\vec{r}, t)$, given on a uniform Cartesian grid. The equation of radiative transfer for the photon number flux N_P [# / s] along a ray reads

$$\frac{\partial N_P}{c \partial t} + \frac{\partial N_P}{\partial r} = -\kappa N_P, \quad (1)$$

where the absorption coefficient $\kappa = \sigma n_H(\vec{r}, t)$ is given from cross-section for photoionization $\sigma \sim 6.3 \times 10^{-18} \text{ cm}^{-2}$

arXiv:astro-ph/0111033v1 1 Nov 2001

at threshold. For simplicity we consider here only photons at threshold. Including the frequency dependency is easily achieved repeating the ray tracing. If the light crossing times are shorter than the opacity time scale $\kappa/\dot{\kappa}$ the time dependent term can be dropped and only the static attenuation equation needs to be solved (ANM99; Norman, Paschos, Abel 1998). The rate of photo-ionizations, $k_P^i(\vec{r})$ [$\text{s}^{-1} \text{cm}^{-3}$], contributed by the i th ray carrying the photon number flux, N_P^i , and passing through a cell with neutral hydrogen density, $n_H(\vec{r})$, for a length, Δr^i , is given by $k_P^i(\vec{r}) = N_P^i(1 - e^{-\tau^i})/(\Delta x^3) = N_P^i[1 - \exp(-n_H(\vec{r})\sigma\Delta r^i)]/(\Delta x^3)$. The total rate of photo-ionization for a given cell is sum of all rays passing through that cell. The number of rays passing through a cell controls the accuracy of the angular integration. Any ray tracing scheme requires of the order $4\pi R^2/(\Delta x)^2$ rays to have at least one ray pass a cell of side length Δx at a distance R from the source. If the number of rays per solid angle is fixed as one traverses the simulation volume, one integrates through cells close to the source unnecessarily more often in order to resolve cells farther away. A similar problem is inherent in Monte Carlo techniques that send photon packages and have to ensure sufficient angular resolution (Ciardi et al. 2001, and references therein).

Using an *adaptive* number of rays overcomes these limitations. We implement this adaptivity by growing a tree of rays out of the point source, subdividing rays locally as they encounter grid cells. The tree can be recombinant, with refinement or coarsening occurring to ensure all cells which are illuminated by the source are traversed by a sufficient number of rays. In the following we discuss how ray directions are chosen.

2.2 HEALPix Pixelization of the sphere

We use the Hierarchical Equal Area isoLatitude Pixelization of the sphere (HEALPix). The details of this pixelization are described in Górski, Hivon, and Wandelt (1998). For our purposes, its advantageous properties are, a) exactly equal area per pixel, b) nearly uniform sampling of solid angle by the pixel centers, c) hierarchical nesting of pixels at different resolutions, and d) the binary **nested** pixel numbering scheme with fast routines provided for converting between pixel numbers and the associated unit vectors.

Figure 1 shows how HEALPix provides a tiling of the sphere with these properties at arbitrarily high resolution by recursively subdividing a set of 12 base pixels. At each refinement step the pixels divide into 4 next-level pixels and thus generate a quad-tree structure. At the l -th level ($l = 0, 1, \dots$), the tiling contains $N_{pix}(l) = 12 \times 4^l$ pixels each of which covers solid angle $A(l) = 4\pi/N_{pix}(l)$. This equal area property ensures equal photon flux per ray for isotropic sources.

This HEALPix quad-tree allows a recursive implementation of an adaptive algorithm for defining a ray tree. Individual rays split into 4^n ($n = 1, 2, \dots$) child rays when necessary to preserve the accuracy of the angular integration. Adopting the **nested** numbering scheme, the numbers of child rays are simply given by adding two bits to the number of the parent rays. This has advantages in memory management and implementation as we will discuss in more detail below.

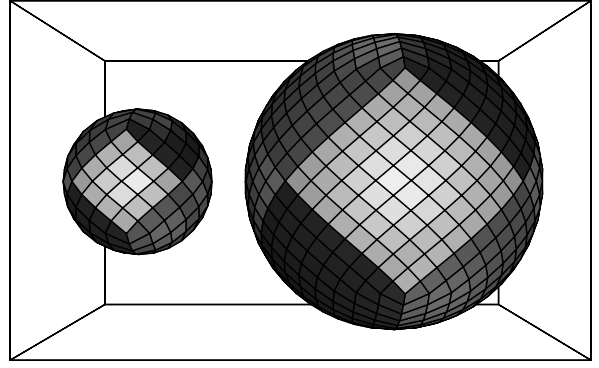


Figure 1. HEALPix pixelization of the sphere. The 12 base pixels are coloured in and shown at resolution $l=2$ (left) and $l=3$ (right). Rays are cast through pixel centers. The hierarchical property of the pixelization enables the efficient construction of a tree of rays (see Fig. 2).

2.3 Splitting Rays and Setting up the Tree

As one walks along a ray a refinement criterion controls whether this ray needs to be broken up into 4 child rays. For the uniform grid the refinement is controlled by keeping $A_c/A(l) > f$. This is the ratio of the area of a cell $A_c = \Delta x^2$ and the area associated with the ray on level l , $A(l) = 4\pi/(12 \times 4^l)$. Here we introduced a safety factor $f \gg 1$ which is the minimum number of rays passing through any cell. We find $f = 2$ to be a good compromise between speed and accuracy. For opacities given on a structured adaptive mesh this refinement criterion is unchanged provided one uses the correct local cell area. For an adaptive smooth particle hydrodynamical representation of the opacities one would use a fraction of the square of the local smoothing length as refinement criterion. The path length through the particle is the line integral through the smoothing kernel.

Once one has decided to split the current ray one determines the four new pixel (ray) numbers by adding two bits to the current ray number. Given the pixel number the HEALPix `pix2vect_nest` routine is used to find the new unit directional vectors for the child rays. The child ray starting points are simply given by the radius of the parent ray times the directional vector. One subtlety is that these starting points may reside in a different cell of the Cartesian grid and hence the associated cell number needs to be recomputed. A tree is realized using two pointers for each ray. We refer to them as `NextRayThisLevel` and `NextRayNextLevel`. As a parent ray splits into child rays it will have `NextRayNextLevel` pointing at the ray number of the first child ray. The first three child rays are created with setting `NextRayThisLevel` to the ray numbers according to their pixel numbering. The last child ray is created with `NextRayThisLevel` pointing to a negative integer value indicating the end of the tree on that level. Given these two pointers per each ray one can quickly walk through the tree of rays. When the ray is split the photon-number flux is equally distributed to the child rays.

Figure 2 gives a graphical illustration of how one base ray is split up into child rays on three additional levels in a uniform grid with only 8 cells on a side.

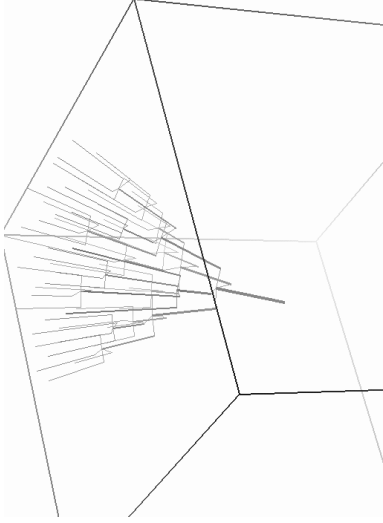


Figure 2. Illustration how one base ray spawns child rays to sample a uniform underlying grid preserving the accuracy of the angular integrations.

2.4 Merging of Rays

For ray-tracing through opacity data with a large dynamic spatial range situations may arise in which it is useful to merge child rays again and start following a new ray of the direction of their parent ray. For a non-uniform Cartesian grid such a criterion is readily specified by again comparing the area associated with the ray to the area associated with the local opacity grid. By keeping $A_c/A(l) < f_M$ one never traces more than f_M rays through any cell. To set up the tree with the merging algorithm one now can set `NextRayNextLevel` of the last of the four child (now parent) rays to point to the merged ray number. `NextRayThisLevel` of that last child (now parent) ray remains set to a negative integer value. If merging is used one also needs to define a flag that remembers that it is merged ray. This flag is needed to evaluate the incoming photon flux of the merged ray from the sum of the outgoing photon fluxes of the 4 parent rays. This setup strategy of the tree is simple to implement, but conceptually not very elegant since merged rays are labeled at a higher level than they really are. However, since this does not affect the efficiency of the integration we do not discuss this here further.

2.5 Ray Ending criteria

In many problems of radiative transfer one can define a simple criterion that justifies to stop tracing rays any further. In our example, the propagation of ionization fronts, it is obvious that one does not need to trace rays after most (e.g. 99%) of the photon flux ($N_P/(12 \times 4^l)$) associated with a ray has been absorbed. This leads to a dramatic reduction of computing expense if only a small fraction of the volume is affected by the radiation. In general, which ray ending criterion is suitable depends on the application at hand.

2.6 Integrating along Rays

The radial integration on Cartesian grids is done identical as explained in detail in ANM99 and we discuss it here only briefly. One simply finds the intersections with the 6 planes containing the faces of the next cell along the x, y, and z coordinates and computes the length of ray segments. The shortest ray segment is the relevant one. In our example problem one then knows the optical depth and hence the photon number flux emerging after the ray has transversed the current ray segment. This in turn gives the corresponding photo ionization rate which is then added to the total photo-ionization rate on the Cartesian grid. In situations where the same radial integration has to be performed multiple times we find it advantageous to store the length of the ray segments and the associated opacity grid indices for each ray.

2.7 Walking through the Tree

One major advantage of the proposed method is the inherent tree structure which allows quick multiple integrations once the tree has been defined. Given the pointers `NextRayThisLevel` and `NextRayNextLevel` which were introduced when the rays were defined the walking through the tree is simple. It is programmed by recursively calling a function that will first integrate the ray then call itself to integrate the ray given by `NextRayNextLevel` pointer and after that the ray recorded by `NextRayThisLevel`. Before, one calls this function to integrate `NextRayNextLevel` one copies the integral quantities (e.g. the photon flux of the ray) to all its child-rays. Alternatively the routine before integrating a ray could copy the integral quantity from its parent. The ray data structure will also need to store a pointer to the parent ray.

3 EXAMPLE

We have tested our scheme on all cases presented in ANM99 and found the results indistinguishable from their non adaptive ray tracing. As a new illustrative example we integrate the radial jump condition of an ionization front in three dimensions.

Consider the simple case of a constant luminosity point source embedded in a static medium of neutral hydrogen. The jump condition along a ray at the location of the ionization front caused by the source reads

$$\frac{N_P}{4\pi R^2} - \int_0^R n^2 \alpha(T) dr = n \frac{dR}{dt}. \quad (2)$$

Here, n , denotes the number density of hydrogen nuclei, $\alpha(T)$, the (in general) temperature dependent recombination rate coefficient, R , the location of the ionization front and N_P the ionizing photon number flux of the source. If we assume the ionized material to have a constant temperature and define $\alpha_4 = \alpha(10^4 \text{ K})$ one can integrate this equation with first order differencing to find the passing time, $t_p(R)$. The ray tracing gives one a list of ΔR_i ray segments from which one finds t_p via

$$t_p^{i+1} = t_p^i + \Delta R_i n(R) \left[\frac{N_P}{4\pi R^2} - \int_0^R n^2 \alpha_4 dr \right]^{-1}. \quad (3)$$

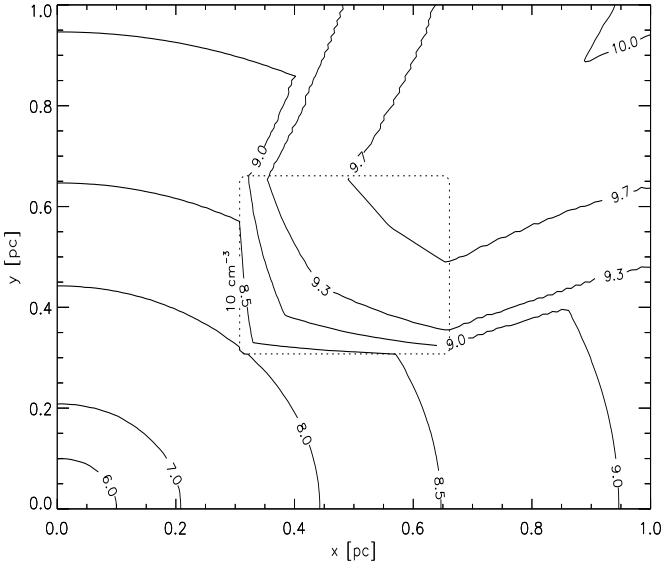


Figure 3. Source of $N_P = 10^{47} \text{ s}^{-1}$ embedded in a uniform medium of $n = 1 \text{ cm}^{-3}$ and a cubic obstacle of ten times higher density ($n = 10 \text{ cm}^{-3}$). The contours give the location of the ionization front at 10^6 , 10^7 , 10^8 , $10^{8.5}$, 10^9 , $10^{9.3}$, $10^{9.7}$ and 10^{10} seconds after the source switched on. The dotted line marks the location of the obstacle. The simulation volume corresponds to side length of one parsec.

The integral of the recombinations from the source to the ionization front is evaluated on the fly. Via this technique one finds the entire evolution of the ionization front in one radial integration. The passing time through a cell is taken to be the maximum passing time evaluated from all rays passing the cell. The classical jump condition gives in the limit of small R a speed of the ionization front dR/dt exceeding the speed of light. To avoid unphysically fast expansion times we therefore limit the maximum Δt_p to be the light crossing time $\Delta R/c$, where, c , denotes the speed of light. The computation is carried out on a uniform Cartesian grid containing 128^3 cells with the source at one of the corners of the grid. We start with $l = 2$ giving 192 base rays. To evaluate all arrival times 1.4×10^5 rays were used. We used a homogeneous initial neutral hydrogen density of 1 cm^{-3} with a cubic obstacle of 10 times larger density and a source with a photon-luminosity of $N_P = 10^{47} \text{ s}^{-1}$. Contours in Figure 3 indicate the ionization front location at different times. A two dimensional slice of the three dimensional volume through the position of the source is shown. The perfect shadowing is evident. Compared to non-adaptive ray tracing this new method is about 20 times faster in this test problem. Using the tree for the integration led in our implementation to a further speed-up of a factor of two. Note, however, that larger speed-ups will be achieved in situations with large dynamic range, where one can stop rays that enter optically thick regions.

4 DISCUSSION

In summary we have presented a novel approach to simulate the effects of radiative transfer around multiple point

sources. The use of adaptive rays with a an inherent tree structure allows significant speed-ups in comparison to uniform ray tracing. Although we have developed it with applications to astrophysical hydrodynamics in mind it is equally well suited for studying static situations and may find application also for volume rendering in computer graphics. The method may also be used for extended emitting sources which are then modeled by a collection of point sources.

It seems clear that generalization of this method may be exploited to speed up Monte Carlo radiative transfer techniques (e.g. Ciardi et al 2001 and references therein). Here one would start with fewer luminous photon packages at the source and split up the the packages to ensure similar number of packages to transverse the numerical grid on which the opacity is defined. This should speed up the calculations significantly since again cells close to the source need not to be accessed more often than any other grid cells.

The adaptive ray tracing scheme suggested in this Letter, allows fast multiple integrations in the case of non-moving sources using a quad-tree. Also, for a variety of problems one may not always have to trace all rays from the source to all other grid cells (or particles). For example, in the case of a thin ionization front penetrating into a high density medium the opacity changes only significantly at the front. Rays need not to be traced far ahead of the front where most of their photons have been consumed. Rays close to the source may also not needed to be traced if their (already low) opacity does not change significantly. Based on this one can formulate a scheme in which rays carry their own opacity time step. As one integrates the chemical rate equations one traces only rays and their child rays which carry an opacity time step less or equal to the current chemical times step. Such a scheme that is also adaptive in time is necessarily more complex and needs to be tailored to the specific problem at hand as well as the method employed for solving the hydrodynamics. We are currently exploring such time adaptive schemes to be implemented for smoothed particle as well as structured adaptive mesh refinement techniques.

ACKNOWLEDGMENTS

T.A. acknowledges stimulating and insightful discussions with Greg Bryan on adaptive numerical schemes and Benedetta Ciardi for comments on the manuscript. This work has partially been supported through NSF grants ACI96-19019 and AST-9803137. T.A. also acknowledge support from the Grand Challenge Cosmology Consortium. B.D.W. is supported by the NASA MAP/MIDEX program.

REFERENCES

- Abel, T., Norman, M.L. & Madau, P. 1999, ApJ, 523, 66 (ANM99)
- Abel T., & Mo H. J., 1998, ApJ, 494, L151
- Barkana, R. and Loeb, A. 2001, Physics Reports in press, astro-ph/0010468
- Ciardi, B., Ferrara, A., Marri, S., Raimondo, G. 2001, MNRAS, 324, 381.
- Gnedin, N. Y., & Abel, T. 2001, ApJ, submitted.
- Górski, K. M., Hivon, E., Wandelt, B. D. 1998, in Proceedings of the MPA/ESO Conference on Evolution of Large-Scale

- Structure from Recombination to Garching; A.J. Banday, *et al*(Eds), astro-ph/9812350. For more details please refer to <http://www.eso.org/kgorski/healpix/>.
- Haehnelt, M.G. 1995, MNRAS, 273, 249
- Haiman, Z., Abel, T. & Madau, P 2000, ApJ, 551, 599
- Kepner, J., Tripp, T. M., Abel, T. & Spergel, D. 1999, AJ, 117, 2063
- Kessel-Deynet, O. & Burkert, A. 2000, MNRAS, 315, 713
- Norman, M. L., Paschos, P., & Abel, T. 1998, in “ H_2 in the Early Universe”, eds. F. Palla, E. Corbelli, and D. Galli, (Mem. S.A.It.), 271
- Razoumov, A. O. & Scott, D. 1999, MNRAS, 309, 287
- Silk, J. & Rees, M. J. 1998, A&A, 331, L1
- Turner, N. J. & Stone, J. M. 2001, ApJS, in press.